

Anomalous dephasing scattering rate of two-dimensional electrons in double quantum well structures

I. R. Pagnossin,^{1,*} A. K. Meikap,^{2,†} T. E. Lamas,¹ G. M. Gusev,¹ and J. C. Portal³

¹*Institute of Physics, University of São Paulo, CP 66318, São Paulo 05315-970, SP, Brazil*

²*Department of Physics, National Institute of Technology, Durgapur, 713209 West Bengal, India*

³*GHMFL-CNRS, BP-166, Grenoble F-38042 Cedex 9, France; INSA, Toulouse 31077 Cedex 4, France;*

and Institute Universitaire de France, Toulouse 31077 Cedex 4, France

(Received 8 May 2008; revised manuscript received 23 August 2008; published 16 September 2008)

The results on the measurement of electrical conductivity and magnetoconductivity of a GaAs double quantum well between 0.5 and 1.1 K are reported. The zero magnetic-field conductivity is well described from the point of view of contributions made by both the weak localization and electron-electron interaction. At low field and low temperature, the magnetoconductivity is dominated by the weak localization effect only. Using the weak localization method, we have determined the electron dephasing times τ_ϕ and tunneling times τ_t . Concerning tunneling, we concluded that τ_t presents a minimum around the balance point; concerning dephasing, we observed an anomalous dependence on temperature and conductivity (or elastic mean free path) of τ_ϕ . This anomalous behavior cannot be explained in terms of the prevailing concepts for the electron-electron interaction in high-mobility two-dimensional electron systems.

DOI: [10.1103/PhysRevB.78.115311](https://doi.org/10.1103/PhysRevB.78.115311)

PACS number(s): 73.63.Hs

I. INTRODUCTION

In the course of the last two decades, it has been established that the constructive interference of phase-coherent electronic waves propagating along a closed path in opposite directions leads to a weak localization (WL) of the conduction electrons. The main experimental signature of this effect is a positive magnetoconductance at low magnetic field due to the breaking of time-reversal symmetry induced by a magnetic field applied perpendicular to the plane of the two-dimensional electron gases (2DEGs). In addition, theoretical modeling allows one to estimate the dephasing time (τ_ϕ) from the experimental magnetoconductivity (MC) of weakly disordered conductors.¹⁻⁴ Furthermore, this work has been extended to high-mobility 2DEG systems during the last decade⁵⁻¹⁴ to determine the dephasing scattering time (τ_ϕ). The electron dephasing time is one of the most important characteristics of semiconductor samples because it sets the rate at which the quantum-mechanical properties of the microscopic system shifts to the classical behavior and also provides information for the microscopic electron-electron and electron-phonon interactions.

Many theoretical and experimental works reported in the literature have established that the electron-phonon scattering is important for three-dimensional systems, whereas the electron-electron scattering is the dominant dephasing process in reduced dimensional systems.¹⁵ So, inelastic electron-electron interaction is the main mechanism of dephasing of the electron wave function in quantum well (QW) structures at low temperature. Theoretical prediction¹⁶ states that the phase scattering rate due to inelastic electron-electron interaction, τ_ϕ^{-1} , is directly proportional to the temperature (T) for the diffusive case ($k_B T \tau / \hbar < 1$, where τ is the elastic-scattering time) and τ_ϕ^{-1} varies directly as $T^2 \ln(2E_F/k_B T)$ for the ballistic case ($k_B T \tau / \hbar > 1$), where E_F is the Fermi energy. This implies that the phase scattering time τ_ϕ diverges at lower temperature ($T \rightarrow 0$). However, a number of experi-

mental groups have shown indications of saturation in τ_ϕ at low temperature. Minkov *et al.*¹⁷ reported the temperature and gate voltage dependences of the phase scattering time. They observed the appearance of saturation of the phase breaking time at low temperature with high positive gate voltage. Studenikin *et al.*⁸ also observed the saturation behavior of τ_ϕ and they concluded that the result could not be satisfactorily described by the Fermi-liquid (FL) theory. But Eshkol *et al.*¹² reported good quantitative agreement of the temperature dependence of the dephasing time with the modified form of the Fermi-liquid theory and they also pointed out that they could not observe any effect of saturation even at the lowest temperature (130 mK) of their measurement. Therefore, experimental efforts have been made to study the electron-electron-scattering time in QW systems and have reached different conclusions.

Apart from a good deal of studies reported in the literature,^{8,12,13,16,17} the behavior of τ_ϕ with elastic mean free path (l_e) in QW systems has not been studied by any experimental method and in particular by the WL method. Therefore, the dependence on the temperature and conductivity (or l_e) of τ_ϕ is of fundamental interest in such highly mobile systems. Information about these dependences is crucial to a profound understanding of the underlying dynamics of the inelastic electron scattering.

It has been established that particles with spin behave differently: a finite spin-orbit coupling introduces random deviations between the spin states of electrons that are back-scattered on time-reversed paths. The resulting spin-space average suppresses the quantum correction to the conductance, given rise to weak antilocalization (WAL), the manifestation of which is a negative magnetoconductance at very low magnetic field. Therefore, the sign of the magnetoconductance would be changed due to the competition of WL and WAL, which gives rise to an antilocalization peak in the magnetoconductance curve at very low magnetic field. Hence, the analysis of the low-field magnetoconductance

could provide quantitative information of the dephasing scattering time (τ_ϕ) and the spin-orbit scattering time (τ_{so}) for high-mobility 2DEG systems.

Raichev and Vasilopoulos¹⁸ investigated the influence of the tunnel coupling between two 2DEG layers in double quantum well (DQW) structures on the WL induced conductivity and magnetoconductivity. This coupling introduces an extra degree of freedom for an electron, like the possibility of tunneling between the layers, which reduces the interference effects. As a result, the WL contribution is reduced as the tunneling rate (τ_t^{-1}) gradually prevails over the dephasing scattering rate (τ_ϕ^{-1}) and it leads to a positive magnetoconductance in the perpendicular magnetic field. Therefore, the analysis of the low-field magnetoconductivity at low temperature by using this model could also provide quantitative information of the tunneling time (τ_t) in addition to the dephasing scattering time (τ_ϕ) in DQW structures.

In this study we have chosen a GaAs DQW system because the weak spin-orbit interaction in GaAs enables us to analyze the measured low-field magnetoconductance data with the modified WL theory proposed by Raichev *et al.*¹⁸ This is done by taking only the dephasing scattering time (τ_ϕ) and the tunneling time (τ_t) as fitting parameters. The spin-orbit interaction is neglected in our analysis due to the following reasons. First, measured magnetoconductivity curves do not show any antilocalization peak at low magnetic field (its presence would indicate a strong spin-orbit interaction). Second, in semiconductor heterostructures, the two mechanisms responsible for the spin-orbit interaction are the structure inversion asymmetry (Rashba term)¹⁹ and the bulk or interface inversion asymmetry (Dresselhaus term).²⁰ According to the structure inversion asymmetry, the spin splitting energy due to the spin-orbit interaction can be expressed as $\Delta = 2\hbar\alpha_0 EK_F$, where α_0 is the Rashba coupling constant, E is the mean electric field in the quantum well, and $K_F = (2\pi n_s)^{1/2}$ is the Fermi wave vector¹⁴ with n_s as the carrier concentration. Using $E \approx 10^5$ V/m, $n_s = 3.22 \times 10^{15}$ m⁻², which is the case for our sample, and taking $a_0 = 5.5$ eV Å² for GaAs,²¹ the calculation yields the value of Δ as 5.4 μ eV. On the other hand, the spin splitting energy due to Dresselhaus spin-orbit coupling for GaAs is around 0.2 meV as calculated by Desrat *et al.*¹⁴ The spin splitting energy¹⁴ is related to the spin-orbit scattering time by the relationship $\Delta = \hbar / \sqrt{\tau_{so}\tau}$. Using this relationship the spin-orbit scattering rate has been calculated separately for Rashba and Dresselhaus contributions. It is observed that the magnitude of the calculated spin-orbit scattering rates (τ_{so}^{-1}) due to both contributions is nearly two to three orders of magnitude smaller than the measured dephasing scattering rate (τ_ϕ^{-1}) or tunneling rate (τ_t^{-1}). Therefore, the contribution of the spin-orbit interaction effect is negligible in our investigated system when compared with the other scattering rates (τ_ϕ^{-1} and τ_t^{-1}) in the WL induced magnetoconductivity.

In the present investigative study, the electrical conductivity and magnetoconductivity of the sample have been measured at low temperature ($0.5 \leq T \leq 1.1$ K) with different gate voltages. The low-field magnetoconductivity is compared with the WL theoretical predictions to determine the values of τ_ϕ and τ_t . Our results for the temperature and conductivity or electron mean-free-path dependences of τ_ϕ and

their implications are described below. It is organized as follows. In Sec. II we give experimental details. Experimental results presented and discussed in Sec. III and concluded in Sec. IV.

II. EXPERIMENTAL TECHNIQUES

The active region of our sample comprises two 14-nm-wide GaAs quantum wells, separated by a 1.4 nm AlGaAs barrier (aluminum concentration of 33.5%). Carriers are provided by two silicon-doped layers (nominal donor concentration equals 4×10^{15} m⁻²), one on each side of the double quantum well structure. The distance from the QW interface to the doped layer—for both wells—is 50 nm, provided by an undoped AlGaAs spacer layer. The sample was grown over a GaAs (001) substrate. In order to avoid depletion of the carriers, a silicon-doped layer was placed close to the surface of the sample (30 nm). The sample was capped with a 10 nm undoped GaAs layer.

The sample was patterned with a four-contact Hall bar (200×500 μ m²) by wet-etching liftoff. Ohmic contacts were obtained by In diffusion across the entire heterostructure (i.e., connecting both wells), while the Au-Ti Schottky front gate was evaporated over the sample surface.

Standard low-frequency lock-in techniques were used (0.1 μ A ac) in order to get the electron concentration and transport mobility by means of the Shubnikov–de Haas (SdH) and ordinary Hall effects. These measurements were carried out in the temperature range $0.5 \leq T \leq 1.1$ K in a ³He bath cryostat with a superconducting coil up to 1 T using magnetic sweep rate as low as 0.02 T/min. In order to vary the conductivity and the electron density (in the QW closer to the surface), we changed the front-gate bias (V_g) from -0.3 to $+0.3$ V.

III. RESULTS AND DISCUSSION

The variation of the diagonal magnetoresistivity (ρ_{xx}) at 0.5 K with perpendicular magnetic field for different gate biases (V_g) is shown in Fig. 1(a). The SdH oscillation patterns show the existence of the two subbands E_1 and E_2 ($E_1 < E_2$) with energy separation $\Delta(V_g, \Delta_{SAS}) = E_2 - E_1$, where Δ_{SAS} is the energy gap between the symmetric and asymmetric states. The densities, n_1 and n_2 , of the lower and upper subbands of the DQWs as a function of V_g are derived by Fourier transforming the SdH oscillations and the results are presented in Fig. 1(b). The balance point of the system is around $V_g = -0.15$ V. A large change is observed in the density of the lower subband n_1 , whereas the density of the upper subband n_2 decreases more slowly with decreasing V_g from $+0.3$ to -0.15 V. Changing V_g mostly changes the lower subband density n_1 , which is localized in the front well. However, a weak decrease in the upper subband density n_2 , which is localized in the back well, is due to the field penetration of the 2DEG.²² Below the balance point ($V_g < -0.15$ V), the lower subband density remains constant, but the upper subband density decreases rapidly. This is because the lower subband is localized to the back well and the upper to the front well. Consequently, changing V_g changes

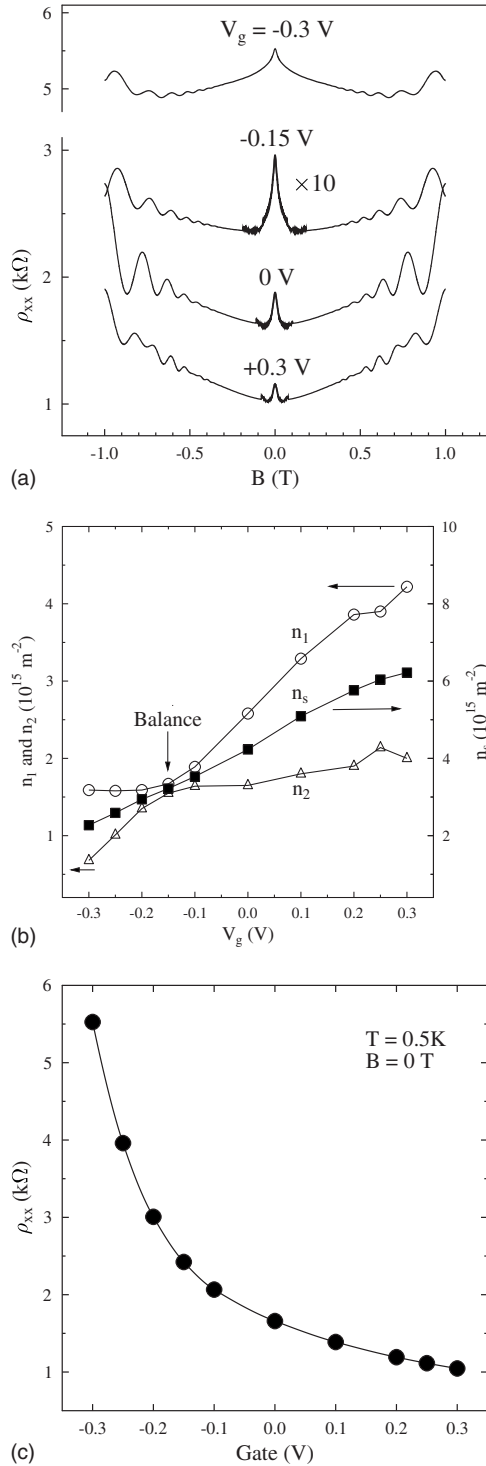


FIG. 1. (a) ρ_{xx} versus B for four different gate bias (V_g) at 0.5 K. Bold data around $B=0$ were amplified for clarity. (b) Experimental n_1 , n_2 , and $n_s (=n_1+n_2)$, obtained from Shubnikov-de Haas and ordinary Hall effects, as a function of V_g . The balance point occurs at -0.15 V. (c) The resistivity as a function of V_g for no applied magnetic field. $T=0.5$ K.

the upper subband density, but could not produce any effect on the density of the lower subband. It should be noted that the total density $n_s=n_1+n_2$ changes approximately linearly with V_g , as is expected from Gauss' law. Figure 1(c) shows

the zero magnetic-field resistivity vs V_g at $T=0.5$ K. The increasing resistivity when V_g is reduced from $+0.3$ to -0.3 V is expected and due to the decrease in the total carrier densities and the increase in scattering rate.

In this study, we also presume that because there is sufficient wave-function delocalization between the two wells as they are separated by a narrow barrier (14 Å), a single layer behavior will be predominant over the entire V_g range, although away from the balance point. As a consequence, we took the total carrier concentration n_s as a reference for the following analysis of the weak localization effect.

Indeed, Davies *et al.*²³ reported the details study on the electron-transport behavior in double-layer electron systems (DLESs). They identified a hybridization of single- and double-layer behaviors in a narrow-barrier DQW by means of magnetoresistivity measurements and Hartree calculations and pointed out two limits: (i) if the system is away from the balance point, the subband wave functions become localized within the individual wells, and (ii) if the system is at the balance point, both subband wave functions are delocalized across both wells. Finally, they concluded that in narrow-barrier DLES they never access true limit (i) behavior because of sufficient wave-function delocalization between the two wells.

In order to gain deeper insight into the electrical transport properties of the investigated sample, we have carefully characterized the temperature dependences of conductivity in zero magnetic field. We find that, at low temperatures, the conductivity of the sample decreases with reducing temperature, which can be explained by taking into consideration the WL and the electron-electron interaction (EEI) effects. After the inclusion of both of these corrections in the diffusive regime ($k_B T \tau / \hbar < 1$), the total conductivity of the system in zero magnetic field can be expressed as

$$\sigma_{xx}(T) = \sigma_{xx}(0) + \Delta\sigma_{WL}(T) + \Delta\sigma_{EEI}(T). \quad (1)$$

The first term is due to classical Drude conductivity, while the second term corresponds to the weak localization, and the third term stands for electron-electron interaction. According to the theory of WL in symmetric double quantum wells under weak spin-orbit interaction,¹⁸ the temperature dependence correction to the conductivity for two-dimensional electron gases in the diffusive region can be expressed by the following equation:

$$\Delta\sigma_{WL}(T) = \frac{e^2}{2\pi^2\hbar} \left[\ln\left(\frac{\tau}{\tau_\phi}\right) + \ln\left(\frac{\tau}{\tau_\phi} + \frac{2\tau}{\tau_t}\right) \right], \quad (2)$$

where τ_ϕ is the average inelastic-scattering time ($\tau_\phi \propto T^{-p}$, where p is a parameter and its value depends on the scattering processes, $p=1-2$ for electron-electron interaction and $p=2-4$ for electron-phonon interaction) and τ_t is the tunneling time.

The correction to the conductivity due to the interaction effect of the two-dimensional electron gas in the diffusive regime can be written as¹⁵

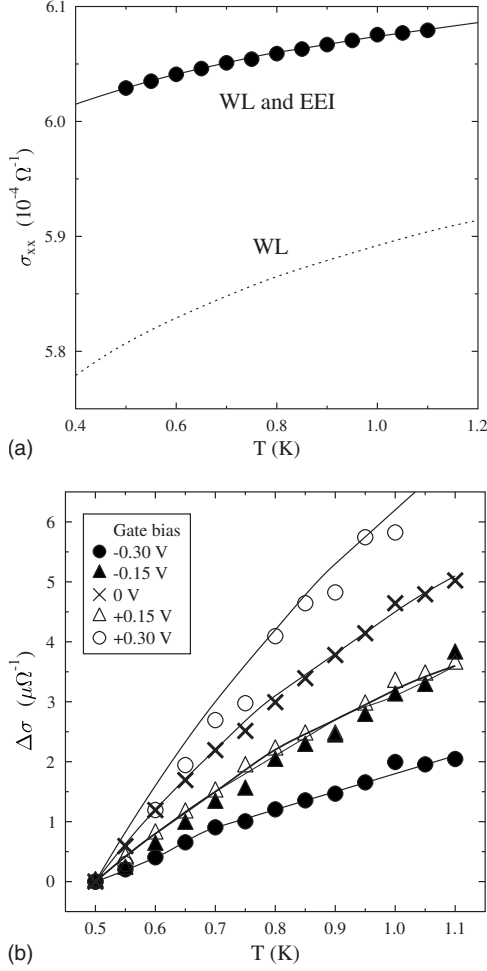


FIG. 2. Variation of the classical conductivity as a function of the temperature for different gate bias. From (a), where $V_g=0$ V, it becomes clear that weak localization alone [dotted line; Eq. (2)] cannot explain the experimental data (symbols): electron-electron interactions are also required [Eq. (3)]. This is true even for $V_g \neq 0$, as shown in (b). $\Delta\sigma = \sigma(T) - \sigma(0.5 \text{ K})$. $B=0$ T in both cases.

$$\Delta\sigma_{\text{EEI}}(T) = \frac{e^2}{2\pi^2\hbar} \lambda \left[\ln\left(\frac{k_B T \tau}{\hbar}\right) \right], \quad (3)$$

where $\lambda = 1 + 3\{1 - [\ln(1 + F_0^\sigma)/F_0^\sigma]\}$ and F_0^σ is the Fermi-liquid interaction constant in the triplet channel, which reflects the strength of the spin exchange interaction.²⁴

The trend of change in conductivity without any application of magnetic field and $V_g=0$ is shown in Fig. 2(a). The points represent the experimental data, while the solid line shows the theoretical fit with Eq. (1) and the dashed line represents the WL contribution alone, which has been drawn by setting $\lambda=0$ and $p=1$. The value of τ_i has been found out from MC analysis (detailed later). We observe from the figure that the theoretical values for only WL contribution did not match with the experimental data, but the total contribution (WL+EEI) is in good agreement with the experimental data for the fitting parameters $F_0^\sigma = -0.653$ and $\sigma_{xx}(0) = 6.267 \times 10^{-4} \text{ } \Omega^{-1}$. The temperature variation of conductivity for different gate biases is shown in Fig. 2(b); the solid

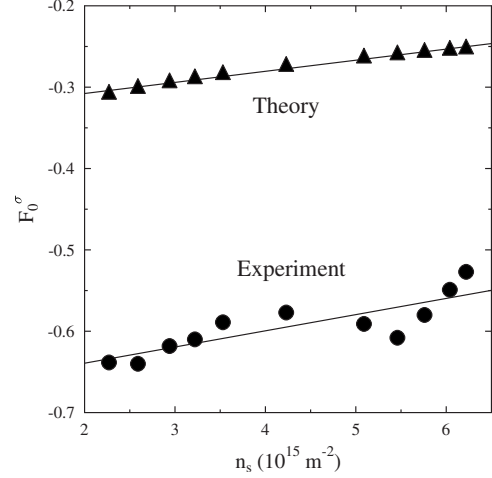


FIG. 3. The interaction parameter F_0^σ as a function of the carrier density (n_s).

lines are the theoretical fit with Eq. (1). Therefore, it may be concluded that in the diffusive regime, both the WL and EEI effects play a dominant role in the low-temperature transport mechanism in the absence of a magnetic field.

We have calculated the values of F_0^σ for different gate voltages from the experimental data by fitting with Eq. (1) and its variation with carrier concentration (n_s) is shown in Fig. 3. Theoretically the value of F_0^σ depends on the parameter r_s by the following equation:²⁴

$$F_0^\sigma = -\frac{1}{2\pi} \frac{r_s}{\sqrt{2-r_s^2}} \ln \left[\frac{\sqrt{2} + \sqrt{2-r_s^2}}{\sqrt{2} - \sqrt{2-r_s^2}} \right] \quad \text{for } r_s^2 < 2, \quad (4)$$

where r_s is the ratio of the Coulomb interaction energy to the kinetic energy and can be obtained by the formula $r_s = \sqrt{2}e^2/\epsilon_s\hbar v_F$, where ϵ_s is the low-frequency dielectric constant and $v_F [= (\hbar/m)\sqrt{2\pi n_s}]$ is the Fermi velocity (m is the effective mass of the electron). The theoretical value of F_0^σ has been calculated by using $\epsilon_s=12.9$ for GaAs and plotted in Fig. 3. It is observed that theoretical and experimental values exhibit a similar trend in behavior with carrier concentration, but the magnitude of the experimental value is almost double the theoretical value.

The magnetoconductivity ($B \neq 0$) for the perpendicular magnetic field was measured within the temperature range $0.5 \leq T \leq 1.1$ K for different gate voltages. The magnetoconductivity is positive for all temperatures and gate voltages and predicts weak spin-orbit scattering for which we did not observe any antilocalization peak.

It was established that both WL and interaction effects make a contribution to the magnetoconductivity at low temperature. The theory of the interaction is used for the case of electron scattering on a point (short range) potential²⁴ or for the case of Coulomb interaction (long range)²⁵ with a scatterer. From the theory of interaction effects, it was shown that the sign and magnitude of the MC would change due to the competitive effects of the Fock and Hartree types of contributions. We have calculated the contribution to the MC due to the interaction effects, as discussed above at low magnetic fields ($B \leq 20$ mT) and low temperature ($T \leq 1.1$ K)

by using the theory in accordance with Zala *et al.*²⁴ and Gornyi and Mirlin.²⁵ We concluded that the calculated MC is about 10^4 times smaller than the experimental data. So, the contribution of the interaction effect at low fields to the MC data is negligible when compared with that of the WL contribution. Therefore, the experimental data can be analyzed only by using the WL theory.

According to the theoretical model for a highly mobile two-dimensional electron gas in double quantum wells, the magnetic-field dependence of the localization correction with respect to the conductivity under diffusive condition ($B < B_{tr}$) is described by the following expression:¹⁸

$$\Delta\sigma_{xx}(B) = \frac{e^2}{4\pi^2\hbar} \left[f\left(\frac{B/B_{tr}}{\tau/\tau_\phi}\right) + f\left(\frac{B/B_{tr}}{\tau/\tau_\phi + 2\tau/\tau_t}\right) \right], \quad (5)$$

where the function $f(x) = \psi(1/2 + 1/x) + \ln(x)$, ψ is the digamma function, and $B_{tr} = \hbar/4eD\tau$ with B_{tr} as the transport field and D as the diffusion coefficient. The variation of magnetoconductivity at different temperatures for zero gate bias is shown in Fig. 4(a) and that at $T=0.5$ K for different gate biases is shown in Fig. 4(b). The symbols represent the experimental data and the solid curves are the theoretical predictions obtained from Eq. (5). So, the WL predictions describe our experimental data well. The average dephasing scattering time τ_ϕ and tunneling time τ_t have been determined from the fits on the plots of MC and the formulas predicted by the WL theories. As expected, we observed that the dephasing scattering time depends strongly on temperature, but the tunneling time is independent of temperature.

In all probabilities, τ_ϕ assumes the role of the determining factor to control the magnitude and temperature dependence of the WL effect. In the absence of magnetic impurities, the phase relaxation originates from inelastic scattering, arising from the contribution of electron-phonon (τ_{e-ph}^{-1}) and electron-electron (τ_{ee}^{-1}) scatterings. On the basis of the theory of electron-phonon interaction,^{26,27} the dephasing rate can be expressed as $\tau_\phi^{-1} \propto T^2/l_e$ for $T \gg \hbar C_t/k_B l_e$ and $\tau_\phi^{-1} \propto T^4 l_e$ for $T \ll \hbar C_t/k_B l_e$, where C_t is the transverse velocity of sound. In order to compare the values of τ_ϕ^{-1} obtained from our experimental data with electron-phonon-scattering rate, we have calculated the value of τ_{e-ph}^{-1} from the theory of electron-phonon interaction by using $C_t = 3 \times 10^3$ m/s of GaAs systems.²⁶ We find that at the highest temperature measured, τ_{e-ph}^{-1} is smaller by approximately 2 orders of magnitude than that of the measured dephasing scattering rate for the investigated sample. The contribution of τ_ϕ^{-1} to the dephasing scattering rate is even less for lower temperatures, which almost rules out any possibility for appreciable contribution from electron-phonon scattering to the dephasing scattering rate. Therefore, the electron-electron scattering dominates in this 2DEG at low temperatures.

According to the FL model,^{15,28,29} the standard result for the electron-electron-scattering rate at high temperature in clean two-dimensional systems ($k_B T \tau / \hbar > 1$) is proportional to T^2 and, at low temperature, it is proportional to T (where small energy-transfer scattering processes dominate). But in all these calculations, only the contribution of the singlet channel interaction (SCI) has been considered. However,

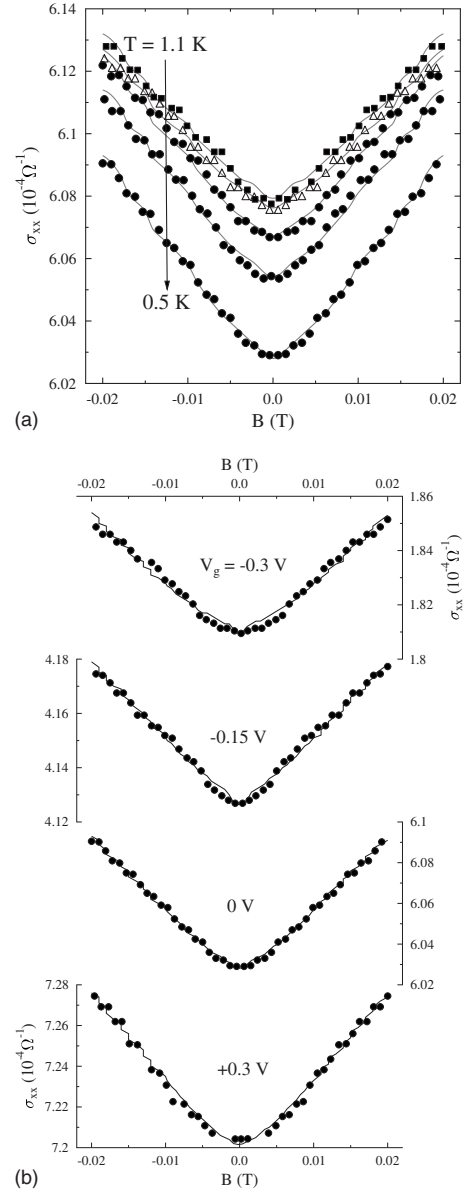


FIG. 4. Magnetoconductivity data as a function of applied magnetic field, perpendicular to the 2DES plane, for (a) $V_g = 0$ and $T = 1.1, 1.0, 0.9, 0.75,$ and 0.5 K (from top to bottom) and for (b) $T = 0.5$ K and different gate biases. The symbols are measured data, while the solid lines are theoretical fits of Eq. (5).

Narozhny *et al.*¹⁶ calculated the dephasing scattering rate including the triplet channel interaction (TCI) in both diffusive and ballistic regimes. According to their theory the temperature dependence of τ_{ee}^{-1} in the small-energy-transfer (SET) scattering processes ($k_B T \tau / \hbar \ll 1$) is given by the following expression:

$$\tau_{ee}^{-1}(T) = \left[1 + \frac{3(F_0^\sigma)^2}{(1 + F_0^\sigma)(2 + F_0^\sigma)} \right] \ln[g(1 + F_0^\sigma)] \frac{k_B T}{g\hbar} + \frac{\pi}{4} \left[1 + \frac{3(F_0^\sigma)^2}{(1 + F_0^\sigma)^2} \right] \frac{k_B^2 T^2}{\hbar E_F} \ln\left(\frac{E_F \tau}{\hbar}\right), \quad (6)$$

where $g = 2\pi\hbar/e^2 R$ is the dimensionless conductance, R is

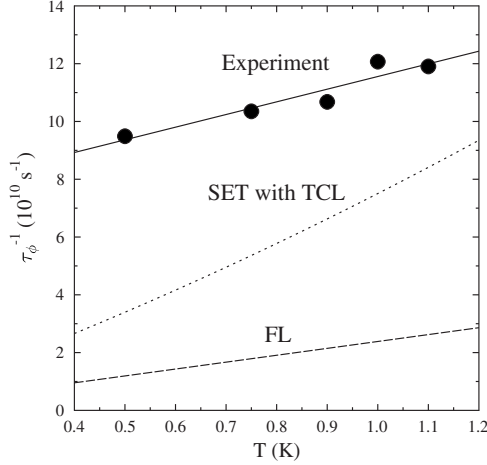


FIG. 5. The dependence of the dephasing scattering rate on the temperature for $V_g=0$. Symbols represent experimental data; the dashed (dotted) line is the calculated behavior from the Fermi-liquid (small energy transfer with triplet channel interaction) model.

the sheet resistance, and E_F is the Fermi energy. Figure 5 shows the variation of the dephasing scattering rate τ_ϕ^{-1} with temperature for zero gate voltage. It is evident from the figure that τ_ϕ^{-1} shows linear temperature dependence. In order to compare the experimentally measured dephasing scattering rate with theory, we have calculated the values of τ_{ee}^{-1} both from Eq. (6) and the Fermi-liquid model^{15,28} by using the values of the parameters (obtained from experimental data of the investigated sample), $F_0^0=-0.653$, $E_F=15$ meV, $\tau=0.34$ ps, and $\sigma_0=2.427 \times 10^{-4} \Omega^{-1}$, and plotted in Fig. 5 as dotted and short-dashed lines, respectively. It is observed from the figure that although the temperature dependence of the experimentally measured dephasing rate is similar to the above theoretical prediction (linear in T), the magnitude did not match with the values calculated from these theories. This discrepancy probably arises due to the anomalous mean free path (l_e) or conductivity (σ) dependence of dephasing scattering time. To clarify this we have also studied the conductivity and mean-free-path dependence, as discussed below.

Figure 6 shows the variation of the dephasing scattering rate with conductivity for a particular temperature $T=0.75$ K. It is observed that τ_ϕ^{-1} increase linearly with increasing conductivity. According to the theoretical prediction (Fermi-liquid model),^{15,28} in two-dimensional systems the main phase breaking mechanism at low temperature is inelastic electron-electron interactions and it has to decrease monotonically with conductivity, which is also shown as a dotted line in Fig. 6. So the conductivity dependence of τ_ϕ^{-1} is in conflict with the theoretical prediction. This anomalous behavior indicates the existence of another mechanism of phase breaking for electrons in the investigated system. In Fig. 7, we have plotted τ_ϕ^{-1} with mean free path (l_e) for the temperatures of 0.5 and 0.9 K. It is observed that τ_ϕ^{-1} also follows a linear variation with l_e having different slopes. The slopes of the curves gradually increase as the temperature also increases, and the variation of slopes (A_l) with temperature is shown in the inset of Fig. 7, which also shows a

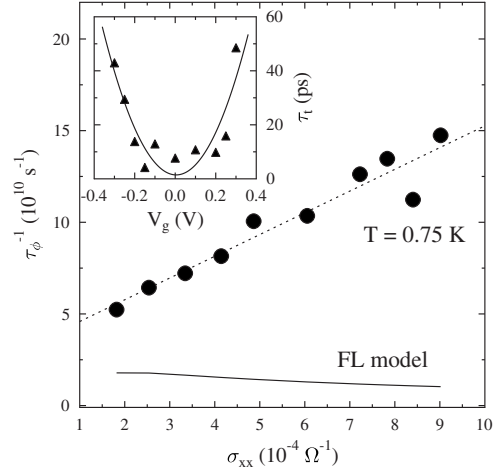


FIG. 6. Dephasing scattering rate versus the conductivity at $T=0.75$ K. The experimental data (symbols), for which $\tau_\phi^{-1} \propto \sigma$, show a clear mismatch with the Fermi-liquid model, for which $\tau_\phi^{-1} \propto \sigma^{-1}$. The inset shows tunneling times for different gate biases.

straight-line variation. From the observation of our experimental result, it may indicate that both contributions (due to conductivity or mean-free-path variation and temperature variation) act together on the dephasing rate, i.e., $\tau_\phi^{-1} \propto \sigma T$ ($\sim T l_e$). This observation cannot be understood in terms of the theory of Fermi-liquid model, where the dephasing scattering rate is expressed as $\tau_\phi^{-1} \propto T/\sigma$ ($\sim T/l_e$). In fact, the linear conductivity or mean-free-path dependence of τ_ϕ^{-1} cannot be explained in terms of any existing theory of electron-electron interaction for impure materials.^{15,16,28,30} So this experimental result may add impetus to the theoretical community to rethink this issue.

In a double quantum well structure, the tunneling between layers gives rise to the closed paths for which an electron starts from one layer, goes to another, and then returns to the first layer. This phenomenon is important when the probability of tunneling is comparable to that of inelastic scattering. The values of tunneling time obtained from MC analysis is

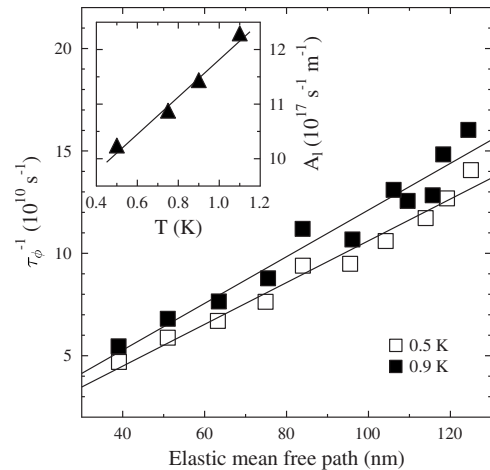


FIG. 7. Dephasing scattering rate versus elastic mean free path for $T=0.5$ K and 0.9 K. The inset shows the correlation of the slopes (A_l) of τ_ϕ^{-1} vs l_e for the temperature range of this study.

comparable with the dephasing scattering (inelastic scattering) time for the investigated sample. The variation of the tunneling time (τ_t) with front gate voltage (V_g) is shown in the inset of Fig. 6. Its value initially decreases with increasing gate voltages and then increases with further increasing gate voltage; i.e., it shows a minimum around the balance point. This behavior indicates that the tunneling rate (τ_t^{-1}) is maximum around the balance point. This is so because by increasing the front gate bias from the balance point to below or above the probability of laying electrons in the back or the front well increases, respectively, due to the increase in the energy difference $\Delta(V_g)$ between the two subbands. As a result, the probability of returning to the original position of an electron by tunneling between the layers gets reduced with respect to the balance point, where the energy difference $\Delta(V_g)$ is minimum.

In view of the effort exerted to understand the mechanism of dephasing scattering in the diffusive limit, it is necessary to see if the experimental data in the present investigation satisfies the diffusive criterion $k_B T \tau / \hbar < 1$. Substituting the values of τ for different gate voltages, the value of $k_B T \tau / \hbar = (0.025 - 0.048)T$, where T is in kelvins. Therefore, it is worth mentioning here that the dephasing processes in the present study meets the diffusive criterion of $k_B T \tau / \hbar < 1$ even at the highest temperature measured. The transport field $B_{tr} = \hbar / 4eD\tau$ was also estimated for different gate voltages and it was found that B_{tr} varies from 21 to 216 mT. Since analysis of MC was done at low magnetic field ($B \leq 20$ mT), the diffusion approximation ($B < B_{tr}$) is satisfied and it can be concluded that the WL theory is well suited to explain the trends shown by the magnetoconductivity in the GaAs system and this enable us to calculate the values of τ_ϕ and τ_t .

IV. CONCLUSION

We have measured the low-temperature electrical conductivity of GaAs (double QW) sample in the absence and in the presence of magnetic field perpendicular to the QW plane for different front gate voltages. Weak localization and electron-electron interaction theories describe the anomalous behavior of zero magnetic-field conductivity data very well. At very low field, the electron-electron interaction contribution to the magnetoconductivity is very small as compared to the weak localization one. The dephasing scattering time and tunneling time have been determined from the low-field magnetoconductivity data using weak localization theory. The tunneling rate is maximum around balance point. We have discussed the temperature and the conductivity (i.e., elastic mean free path) dependence of τ_ϕ^{-1} . Our results reveal a linear temperature behavior, i.e., $\tau_\phi^{-1} \sim T$, which can be described by the electron-electron interaction due to small-energy-transfer processes. Moreover, our results indicate a linear conductivity or elastic mean-free-path dependence, i.e., $\tau_\phi^{-1} \sim \sigma$ or $\tau_\phi^{-1} \sim l_e$, which contradicts the Fermi-liquid model and whose origin is still unknown. So our results, $\tau_\phi^{-1} \sim \sigma T$ ($\sim T l_e$), should make us rethink previous theories which have been taken for granted concerning electron-electron scattering in highly mobile two-dimensional electron gas.

ACKNOWLEDGMENTS

Support of this work by FAPESP and CNPq (Brazilian agencies) is thankfully acknowledged. A.K.M. thanks the FAPESP for providing all kind of financial support including his travel and sustenance allowances.

*irpagnossin@usp.br

†meikapnidd@yahoo.com

- ¹E. Abrahams, P. W. Anderson, D. C. Licciardello, and T. V. Ramakrishnan, Phys. Rev. Lett. **42**, 673 (1979).
- ²P. W. Anderson, D. J. Thouless, E. Abrahams, and D. S. Fisher, Phys. Rev. B **22**, 3519 (1980).
- ³S. Hikami, A. I. Larkin, and Y. Nagaoka, Prog. Theor. Phys. **63**, 707 (1980).
- ⁴G. Bergmann, Phys. Rep. **107**, 1 (1984).
- ⁵S. V. Iordanskii, Y. B. Lyanda-Geller, and G. E. Pikus, Pis'ma Zh. Eksp. Teor. Fiz. **60**, 199 (1994); [JETP Lett. **60**, 206 (1994)].
- ⁶A. Zduniak, M. I. Dyakonov, and W. Knap, Phys. Rev. B **56**, 1996 (1997).
- ⁷N. S. Averkiev, L. E. Golub, and G. E. Pikus, Semiconductors **32**, 1087 (1998).
- ⁸S. A. Studenikin, P. T. Coleridge, N. Ahmed, P. J. Poole, and A. Sachrajda, Phys. Rev. B **68**, 035317 (2003).
- ⁹J. B. Miller, D. M. Zumbuhl, C. M. Marcus, Y. B. Lyanda-Geller, D. Goldhaber-Gordon, K. Campman, and A. C. Gossard, Phys. Rev. Lett. **90**, 076807 (2003).
- ¹⁰G. M. Minkov, A. V. Germanenko, O. E. Rut, A. A. Sherstobitov, L. E. Golub, B. N. Zvonkov, and M. Willander, Phys. Rev.

B **70**, 155323 (2004).

- ¹¹L. E. Golub, Phys. Rev. B **71**, 235310 (2005).
- ¹²M. Eshkol, E. Eisenberg, M. Karpovski, and A. Palevski, Phys. Rev. B **73**, 115318 (2006).
- ¹³N. Thillosen, S. Cabanas, N. Kaluza, V. A. Guzenko, H. Hardt-degen, and Th. Schapers, Phys. Rev. B **73**, 241311(R) (2006).
- ¹⁴W. Desrat, D. K. Maude, Z. R. Wasilewski, R. Airey, and G. Hill, Phys. Rev. B **74**, 193317 (2006).
- ¹⁵B. L. Altshuler and A. G. Aronov, in *Electron-Electron Interactions in Disordered Systems*, edited by A. L. Efros and M. Pollak (Elsevier, Amsterdam, 1985).
- ¹⁶B. N. Narozhny, G. Zala, and I. L. Aleiner, Phys. Rev. B **65**, 180202(R) (2002).
- ¹⁷G. M. Minkov, A. V. Germanenko, O. E. Rut, A. A. Sherstobitov, B. N. Zvonkov, E. A. Uskova, and A. A. Birukov, Phys. Rev. B **64**, 193309 (2001).
- ¹⁸O. E. Raichev and P. Vasilopoulos, J. Phys.: Condens. Matter **12**, 589 (2000).
- ¹⁹E. I. Rashba, Fiz. Tverd. Tela (Leningrad) **2**, 1224 (1960) [Sov. Phys. Solid State **2**, 1109 (1960)].
- ²⁰P. D. Dresselhaus, C. M. A. Papavassiliou, R. G. Wheeler, and R. N. Sacks, Phys. Rev. Lett. **68**, 106 (1992).
- ²¹G. Lommer, F. Malcher, and U. Rossler, Phys. Rev. Lett. **60**,

- 728 (1988).
- ²²S. Luryi, *Appl. Phys. Lett.* **52**, 501 (1988).
- ²³A. G. Davies, C. H. W. Barnes, K. R. Zolleis, J. T. Nicholls, M. Y. Simmons, and D. A. Ritchie, *Phys. Rev. B* **54**, R17331 (1996).
- ²⁴G. Zala, B. N. Narozhny, and I. L. Aleiner, *Phys. Rev. B* **64**, 214204 (2001).
- ²⁵I. V. Gornyi and A. D. Mirlin, *Phys. Rev. Lett.* **90**, 076801 (2003).
- ²⁶J. Rammer and A. Schmid, *Phys. Rev. B* **34**, 1352 (1986).
- ²⁷S. Iordanski and Y. Levinson, *Phys. Rev. B* **53**, 7308 (1996).
- ²⁸B. L. Altshuler, A. G. Aronov, and D. E. Khel'nitskii, *J. Phys. C* **15**, 7367 (1982).
- ²⁹W. E. Eiler, *J. Low Temp. Phys.* **56**, 481 (1984).
- ³⁰M. Kaveh and N. Wiser, *Adv. Phys.* **33**, 257 (1984).